Surface-enhanced Raman Spectroscopy of Biological System

Mustafa Culha

Prof. Culha is currently a Professor of Chemistry at Augusta University. He obtained his MS degree from Wake Forest University, NC, in 1997 and his Ph.D. at the University of Tennessee-Knoxville in 2002. Then, he joined in Advanced Biomedical Research Group as a post-doctoral researcher at Oak Ridge National Laboratory (2002-2003) before joining to Schering-Plough Corporation, NJ as an investigator. He accepted a faculty potion at Yeditepe University, Istanbul, Türkiye, in 2004 and he involved in research and teaching at Genetics and Bioengineering Department more than 14 years. Then, he spent one and half years at The Knight Cancer Institute's Cancer Early Detection Advanced Research center (CEDAR) at Oregon Health and Science University as a visiting scientist. His current research interest includes elements from chemistry, medicine, material science, photonics, and nanoscience and nanotechnology. One of his major research directions is the biomedical applications of surface-enhanced Raman scattering (SERS). He and his colleagues have authored of more than 130 papers in refereed international journals, several book chapters and patents in the areas of analytical and bioanalytical chemistry, and nanobiotechnology. He is also the president elect for The Federation of Asian Chemical Societies (FACS) for the 2023-2025 term.

Ertug Avci

Ertug Avci received his bachelor's degree from Molecular Biology and Genetics Department, Boğaziçi University, Türkiye in 2008, and got his MSc degree at Biotechnology Program of Yeditepe University in 2010. He continued his research in the same department and got his PhD in 2019. He was a postdoctoral researcher at Sabancı University Research and Application Center, Türkiye in November 2022-April 2023. Currently, he is a postdoctoral researcher at Department of Chemistry and Biochemistry, Augusta University, USA. His research work focuses on surface-enhanced Raman spectroscopy of liquid biopsy, biological molecules, and cells.

By: Ertug Avci and Mustafa Culha

https://doi.org/10.51167/acm00064

Surface-enhanced Raman spectroscopy (SERS), a vibrational spectroscopy technique, enables label-free detection, identification, and discrimination of biological structures such as proteins, microorganisms, and cells on nanostructured noble metal surfaces such as gold and silver through chemical and electromagnetic enhancement mechanisms. In this review, a brief introduction to Raman scattering and SERS are given. Then, the SERS applications on proteins, microorganisms, and cells performed by our group are discussed.

Raman scattering

As well known, in the last a few decades of the 19th century and the first decades of the 20th century, the world welcomed many breakthroughs in the field of physics. One of the main contributors to the field was John William Strutt (Lord Rayleigh). He discovered the physical explanations of why the sky is blue.[1-3] He observed that molecules in the atmosphere scatter the incident sunlight. This type of scattering is now called as Rayleigh scattering. Lord Rayleigh analyzed the blue-sky phenomenon using James Clerk Maxwell's equations for the electromagnetic field in detail; he found that intensity of scattered radiation varies inversely with the fourth power of the wavelength.[4,5] This meant that shorter blue wavelengths in the sun light would be scattered more efficiently than the longer red wavelengths. Rayleigh also interpreted the color of sea as the reflection of the color of the sky.

After three years of Rayleigh's death, in 1922, another brilliant young scientist, Chandrasekhara Venkata Raman, reported that sea was also scattering the light.[6] Later, Raman started investigating the light scattering phenomenon more intensively with his colleagues in Calcutta, India.

In 1923, Arthur Compton showed that scattered X-rays from electrons of a carbon sample had longer wavelengths than those targeted onto the sample.[7] In his experiments, both electrons and scattering X-rays went separate ways upon collusion while scattering X-rays had longer wavelengths (e.g., a ball "A" hits another ball "B", and incoming ball goes in a different direction while losing its energy). Compton thought that this was due to conservation of energy and momentum, and photons may be considered as particles. This was the first demonstration of inelastic scattering. In 1927, Compton was awarded with the Nobel Prize in Physics for this discovery.

Meanwhile Raman was studying on the nature of light scattering on various media such as liquids, gases, and crystals, and trying to understand the nature of so called "secondary radiations", and their difference from fluorescence. He suspected that the findings could be due to fluorescence originating from impurities in liquids, therefore he further purified chemicals to avoid fluorescence contribution in his experiments. What he found that the secondary radiation (the scattering light through liquids upon illumination with sunlight) was polarizing. This was very important because most of the fluorescence was unpolarized radiations. On the other hand, power of light was not sufficient to obtain higher efficiencies in his experiments; therefore, this new type of scattering could be observable only on a few liquids. After Compton's findings, he thought that his and his colleague's findings might be analogous to that of Compton's. That time, he used optic parts of a telescope to be able to obtain stronger sunlight for his studies on scattering, and purified the liquids by repeated distillation in vacuum environment. He used around 80 different liquids to prove universality of the new type of scattering. Later, he used monochromatic light source for further experiments. For each liquid, on spectrograms, he observed additional lines present on the right side of the lines occurred due to incident light, meaning that those additional lines had longer wavelengths. Findings of these experiments were published in the journal Nature having a title "A new type of secondary radiation" on 31st March 1928.[8] This new type of scattering is now called as Raman scattering. C.V. Raman received a Nobel Prize in 1930 for his valuable contributions to the field of physics.

Rayleigh and Raman scatterings can be explained further on a Jablonski diagram (Figure 1a). Scattering can be thought of as a two-photon process. During Rayleigh scattering process, a molecule absorbing energy of photons cannot reach an excited electronic state, therefore the state where a molecule reaches is called a virtual state. Then, the energy level of the molecule comes back down to its initial ground state while emitting the absorbed energy. Therefore, the energy of the emitted photon (therefore also its wavelength) is equal to the energy of the incident photon. During Raman scattering, a molecule reaches a virtual state, and then returns to a final state which is different from its initial state. Therefore, the frequency and the energy of the emitted photon become different from the incident photon. If the scattered photons possess less energy from the incident photons, this type of scattering is called Stokes scattering (Figure 1a). If the inverse happens, then it is called anti-Stokes scattering. In a scattering event, Rayleigh scattering comprises more than 99.9 per cent of total scatterings. The other two, Stokes and anti-Stokes comprise extremely small portion (~10^{-7}) of scattered photons. Since most of the molecules resides somewhere close to their ground state energy level at room temperature, intensity of Stokes scattering is higher than anti-Stokes scattering.

Stokes and Anti-Stokes scattering are presented in Raman spectrum plots as Raman shift values, which are shown in terms of wavenumbers rather than wavelength values. Wavenumber of a Raman shift value is found using the following equation:

$$Raman\ shift\ (cm^{-1}) = \left(\frac{1}{\lambda_{incident\ light}} - \frac{1}{\lambda_{scattered\ light}}\right) x10^{7}$$

According to the equation, wavenumber values for Stokes scattering are positive values, because their wavelengths are longer than the incident light. On the other hand, for Anti-Stokes scattering, wavenumber values are negative. Figure 1b shows a typical Raman spectrum plot. The intensity values of the Raman bands are shown in arbitrary units. Although Stokes scatterings are preferred due to their higher intensity, both types can be used in research and development with the use of special filter system (edge vs notch) built in a Raman Spectrometer.

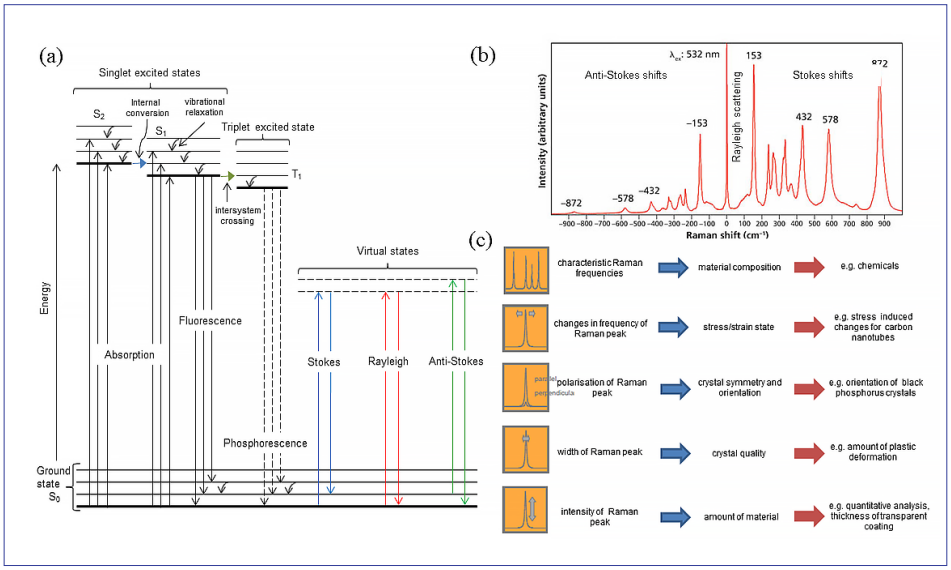

Figure 1. (a) Jablonski diagram of energy transitions for absorption, fluorescence, phosphorescence, Rayleigh scattering, and Raman scattering (Stokes scattering and anti-Stokes scattering). (b) Stokes and anti-Stokes shift of a LiBNO3 single crystal (adapted from ref. 9), (c) Information obtained from a Raman spectrum.

Raman spectroscopy is a versatile technique for various types of research because a Raman spectrum can provide valuable molecular information about a sample (Figure 1c). Since each chemical bonds possess different vibrational energies, the scattered light from each of them differs. Therefore, a Raman spectrum of a molecule has a distinct spectral pattern making them a "fingerprint". With this feature, a Raman spectrum from a gas, liquid, and solid sample can provide a wealth of molecular information.

Plasmonics

Plasmon word comes from unification of the Greek word "plasma" and "mons". Plasma means molded or shaped, and mons means a mountain or body. In physics, the model of a conductor is an array of metallic ions surrounded by a sea of electrons, which is called "free electron gas". Plasmon is a quasi-particle that can be described by a collection of interacting particles and conduction electrons make up the free electron gas.[10] In other terms, electron gas around nanostructures oscillates collectively and a plasmon phenomenon occurs around them. When these plasmons occurs at the interface between metal and dielectric surface, it is called "surface plasmons".[11] There are two types of surfaces plasmons: propagating ones and non-propagating ones. The latter one is called "localized surface plasmon" (LSP) and occurs around nanometer sized noble metals due to confinement of plasmons.[12] In the visible region of the spectrum, the wavelength of light is much larger than the size of a nanoparticle. When the visible light interacts with a nanoparticle, the external electric field of light creates a distortion in the electron cloud that makes up the surface plasmons. If nanoparticles are excited at a resonant frequency, the absorption of light and the response of the nanoparticles become very strong, and this time it is called "localized surface plasmon resonance" (LSPR). The light wavelength at which LSPR occurs depends on size and shape of nanoparticles, aggregation state of nanoparticles, and refractive index of the environment surrounding the nanoparticles.[13-14]

Surface-enhanced Raman scattering

Surface-enhanced Raman scattering (SERS) can be defined as the much more enhanced Raman scattering from molecules when they are either adsorbed on or brought in close vicinity of noble metal nanoparticles such as gold nanoparticles (AuNP) and silver nanoparticles (AgNP).[15] This type of enhanced Raman scattering was first observed in 1974 by Fleischmann et al. while studying with pyridine on roughened silver electrode surfaces.[16] Three years later, in 1977, Van Duyne and his graduate student Jeanmaire found that the reason for 10^5-10^6 times enhanced Raman scattering might not only be due to the surface roughness of the electrode, and stated that there must have been other factors causing the enhanced Raman scattering, and electric field enhancement could be the reason for this phenomenon.[17] In the same year, a separate group of Albrecht and Creighton reported "Anomalously Intense Raman Spectra of Pyridine at a Silver Electrode".[18] They proposed that enhanced Raman scattering was due to a charge transfer between surface and adsorbed pyridine molecules resulting in a resonance Raman scattering. This finding is now accepted as "chemical enhancement theory of SERS". After these findings, Van Duyne met and discussed with physicists, learned from them more about surface plasmons, and developed "electromagnetic field enhancement theory of SERS".[19] Today, both chemical enhancement theory and electromagnetic theory are accepted as the contributors of SERS theory.

As it was discussed in the previous section, a localized surface plasmon resonance occurs on noble metal nanoparticle surfaces in the presence of an electromagnetic field. When Raman scattering molecules come nearby of these nanoparticles, their induced dipole moments increase, therefore the amount of Raman scattering from that molecule increases. The highest enhancements occurs when molecules are present between adjacent nanoparticles due to a "hot spot" formation between adjacent nanoparticles (i.e., when the distance between nanoparticles is less than 4 nanometer).[20] Generally, in a SERS experiment, more than 25 per cent of total enhancement (in many cases more than 50 per cent) are obtained from the molecules in the hot spots, although total surface area of the hot spots are less than one per cent of the total surface of the nanoparticles interacting with a light source.[21] This extreme intensity increase in hot spots even makes single molecule detection possible.[22]

The major parameters in a SERS experiment are laser frequency/wavelength, SERS substrate type (i.e., colloidal AgNPs, AuNPs or solid substrates, size, shape, and surface chemistry of nanoparticles, and aggregation status of nanoparticles. All these parameters are interconnected. Intensity of the SERS bands may differ with the wavelength of laser. Some laser wavelengths may be more suitable for some molecules. Especially, fluorescence may be a problem with visible wavelengths while dealing with biological molecules. The use of a near infrared (NIR) laser mostly overcomes this problem. Size and shape of nanoparticles effect surface plasmon formation as well. Further, NP surface chemistry defines interaction of the molecules with nanoparticle surface. For example, positively charged molecules can interact better with a negatively charged nanoparticles than the negatively charged molecules. In addition, the molecules possessing certain functional groups such as amines and thiols can bind easily to noble metal nanoparticle surfaces. Molecule orientation on the nanoparticle surface also effects the shape of obtained spectra, because the Raman scattering of the chemical bonds which are the nearest to the nanoparticle surface is more enhanced. The aggregation status of nanoparticles is directly linked to hot spot formation. More aggregated colloidal nanoparticles may produce more hot spots, hence produce higher SERS signals. On the other hand, direction of accumulation of nanoparticles during aggregation should be perpendicular to impinging laser.[23] The direction of hot spot formation and chaotic nature of aggregation can be resolved by using solid patterned SERS substrates. On the other hand, production of these type of substrates are costly and time consuming. In addition, since they are contaminated within an experiment, they are not reusable. As seen, there are always trade-offs among different options, therefore a SERS experimenter must choose a proper laser wavelength and substrate for his/her "specific experiment".

In the following sections, the SERS applications on proteins, microorganisms, and cells performed by our group are discussed.

Proteins

Raman spectroscopy is one of the techniques utilized for protein detection and identification. With its nondestructive nature and low sensitivity to water, it can provide fingerprint information from proteins. However, Raman scattering is an inherently very weak phenomenon, and Raman scattering from proteins is very inefficient due to their chemical structure. Enhancement of Raman scattering of proteins on noble metal surfaces drastically lowers the detection limits for proteins and has been used since the 1980s.[24] In order to familiarize the readers with typical SERS spectra of proteins, spectra of eight different blood proteins are shown in Figure 2a. The spectra were acquired using an 830 nm near-IR (NIR) laser after mixing proteins with a suspension of AgNPs with an average size of 50 nm and drying of the mixture. Human serum albumin (HSA) accounts for 55 % of blood plasma proteins. Globulins are the second prevalent proteins with 30–40 % abundance. Fibrinogen (Fb), a blood clotting protein, makes up around 5 % of

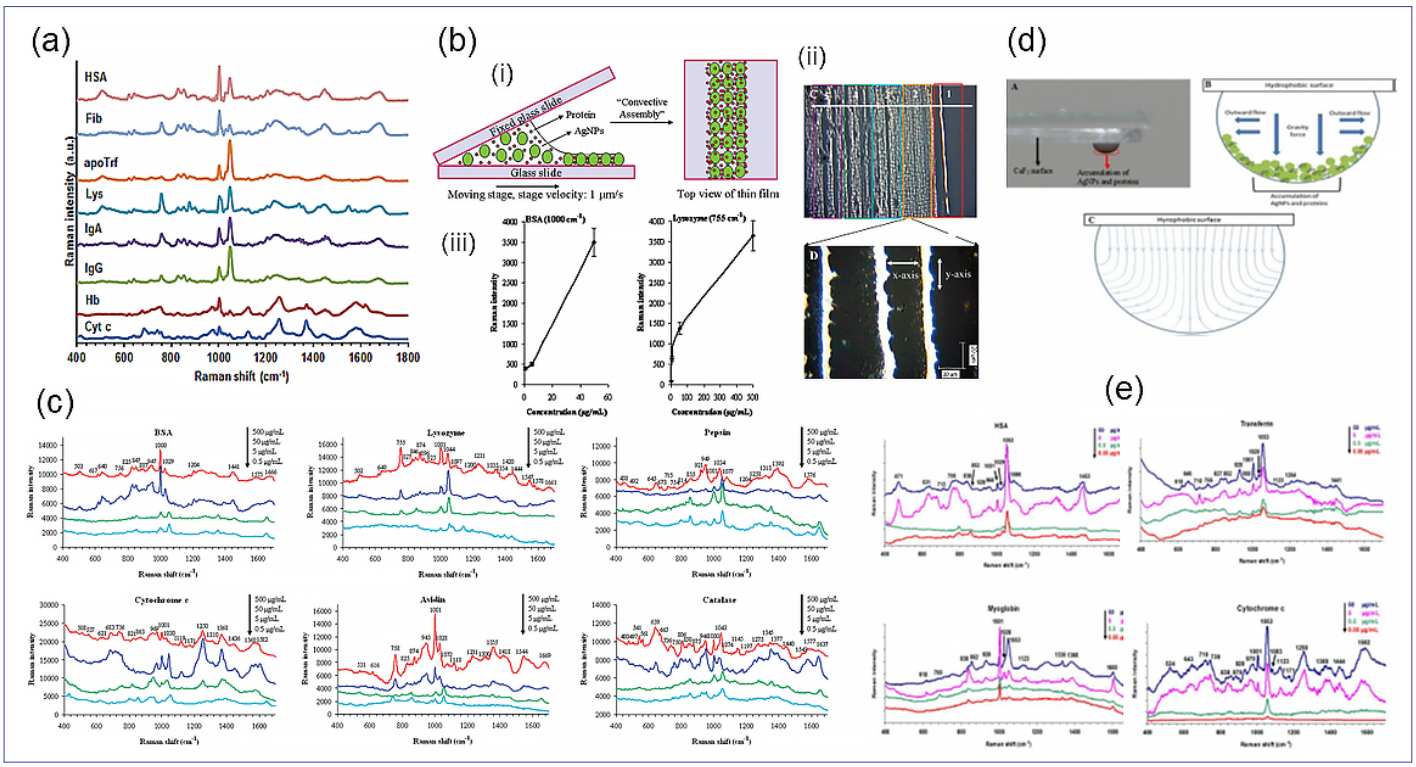

Figure 2. (a) Label-free SERS spectra of human serum albumin (HSA), fibrinogen (Fib), apotransferrin (apoTrf), lysozyme (Lys), immunoglobulin A (IgA), immunoglobulin G (IgG), hemoglobin (Hb), cytochrome c (Cyt c) (adapted from ref. 27). (b) Systematic illustration of the convective assembly process of protein/AgNPs mixtures (i), white light images of the thin film prepared with BSA under 5× objective and 50x objective (ii), dependence of SERS intensity on BSA and lysozyme concentrations (iii) (adapted from ref. 28). (c) SERS spectra of BSA, lysozyme, pepsin, cytochrome c, avidin, and catalase with their decreasing concentration in AgNP colloidal suspension (adapted from ref.28). (d) Photograph and schematic illustration and solvent flow projection of AgNP and protein containing suspended drying droplet on CaF2 surface (adapted from ref. 30). (e) SERS spectra of HSA, transferrin, myoglobin, cytochrome c with their decreasing concentration (adapted from ref. 30).

blood plasma proteins. Transferrin (Trf) is an iron transporter protein and covers a similar percentage of blood proteins as fibrinogen.

As seen in the figure, proteins have similar SERS bands. This is expected because proteins are composed of different combinations of the same 20 amino acids, and these amino acids bind each other with the same peptide bond, which is an amide bond. Structural and functional differences among proteins stem from having different combinations of these amino acids. In label-free SERS, these differences are directly reflected in their spectra. The numbers of each amino acid and the position of each amino acid in the 3D protein structure define the final detail of the spectrum. At first glance, it is seen that SERS spectra of hemoglobin (Hb) and cytochrome c (Cyt c) are quite different from the spectra of other proteins. This is because of the presence of a heme group in their structure. The heme group is composed of a porphyrin ring having an iron ion in its center and has a distinct Raman and SERS spectrum.[25] Its SERS spectrum suppresses the SERS signals of amino acids. For nonheme proteins, Raman bands between 400 cm^{-1} and 1200 cm^{-1} stem from amino acids.[26] Mostly aromatic amino acids (phenylalanine (Phe), tyrosine (Tyr), and tryptophan (Trp)) contribute to the spectrum. Bands between 1200 and 1800 cm^{-1} are mainly due to the backbone structure of the proteins. The distribution of α-helices and β-sheets in the 3D structure of proteins defines the shape of this part of a protein spectrum.

Kahraman et al. reported a simple and sensitive label-free protein detection method based on assembly of proteins and colloidal silver nanoparticles (AgNPs) on surfaces and SERS.[27] The "convective assembly" process which involves the assembly of micro- and nanometer size particles from an evaporating meniscus of an aqueous suspension was used to assemble proteins and AgNPs in an ordered way (Figure 2b). A 40 μL of mixture with proteins and AgNPs was spotted at the junction of two glass slides with a micropipette. The angle between two slides was about 23°. The velocity of the bottom stage was set to 1.0 μm/s for all measurements. Then, SERS spectra from dried thin films were acquired. The SERS spectra from the assembled AgNP/protein films show excellent reproducibility and high quality regardless of the proteins' charge status and size. A detection limit down to 0.5 μg/mL for three acidic proteins; BSA, catalase and pepsin, and three basic proteins; cytochrome c, avidin and lysozyme, is easily achieved. The minimum improvement in detection limit is more than 1 order of magnitude compared to the previously reported detection limits using the technique and the approach has the potential for label-free protein detection and identification. In order to evaluate response signal versus concentration relationship, the intensity of the bands at around 1000 cm^{-1} originating from Phe for BSA and 755 cm^{-1} originating from Trp for lysozyme was plotted against their concentrations in the colloidal suspension. Figure 2biii shows the concentration-dependent SERS intensities of BSA and lysozyme. The other proteins used in the study showed similar intensity versus concentration curves and the approach reported in this study can be used for quantification of proteins.

Keskin et al. applied convective assembly method for differential separation of protein mixtures using label-free SERS detection. Binary mixtures of IgA-hemoglobin and cytochrome c-avidin, and ternary mixtures of IgA-HSA-insulin were used to show applicability of the method.[29] Euclidian distance plots of the acquired spectra from various places along deposited thin films demonstrated a

differential separation of proteins. In another study, Keskin et al. used suspended droplet method for label-free detection of proteins (Figure 2d).[30] This method overcomes the problems that result with the jamming of all species at the liquid-solid contact of a drying sessile droplet (coffee ring phenomenon). A mixture of proteins and AgNPs were spotted on hydrophobic CaF_2 slides and dried for SERS spectra acquisition. A suspending droplet from a hydrophobic surface alters the dynamics in the droplet during evaporation. The use of a hydrophobic surface prevents the spread of the droplet and keeps the droplet confined as much as possible. The protein-AgNP clusters formed in the middle of the droplet area were found suitable for successful SERS measurements. Six different proteins with different size and surface charge properties (HSA, transferrin, myoglobin, cytochrome c, avidin, and lysozyme) were selected as models to test the approach. It was possible to detect down to 0.05 µg/mL protein concentration without the need for an added label (Figure 2e). Avci et al. showed influence of protein size on SERS spectra in binary protein mixtures.[27] The size-dependent interactions of eight blood proteins with AgNPs in their binary mixtures (lysozyme-apotransferrin, cytochrome c-hemoglobin, HSA-fibrinogen, IgG-IgA) were investigated using SERS. Total protein concentrations in the mixtures were 1 µM and concentration of each protein in the binary mixture varied from 0 to 1 µM with 0.2 µM increments. Principal component analysis (PCA) was performed on the SERS spectra of each binary mixture, and the differentiation ability of the mixtures was tested. It was found that the effect of relative concentration change on the SERS spectra of the binary mixtures of small proteins could be detected using PCA. However, this change was not observed with the binary mixtures of large proteins. This study demonstrated that the relative interactions of the smaller proteins with an average size of 50 nm AgNPs smaller than the large proteins could be monitored, and this information can be used for the detection of proteins in protein mixtures.

Microorganisms

Detection and identification of pathogenic microorganisms continue to be a challenge in medical, environmental, and pharmaceutical samples. Once a pathogenic microorganism enters the food chain or the environment through terrorism or another route, it may cause great damage to human health and the environment. SERS technique has been used as an identification, detection, and differentiation method for microorganisms. Kahraman et al. investigated the parameters required for reproducible SERS spectra of bacteria on aggregated AgNPs.[31] A simple sample preparation method was demonstrated. Cultured E. coli and B. megaterium cells were washed with deionized water three times, and 5 µL of the microorganisms were mixed with 100 µL AgNP colloids. Five µL of this mixture was deposited onto a CaF2 slide and dried at room temperature for 15–30 min before SERS analysis. It was found that reproducibility of acquired spectra with a 830 nm laser were better than that of 514 nm laser. The effect of the pH on the spectra were investigated. A pH change influences the ionization status of the functional groups on the amino acid moieties, such as amino and carboxylic acid on the bacterial cell walls. Any change in the surface charges of AgNPs may influence the type of interaction depending on the ionization status of the ionizing group and electrostatic interaction between nanoparticles and the bacterial cell wall. There were

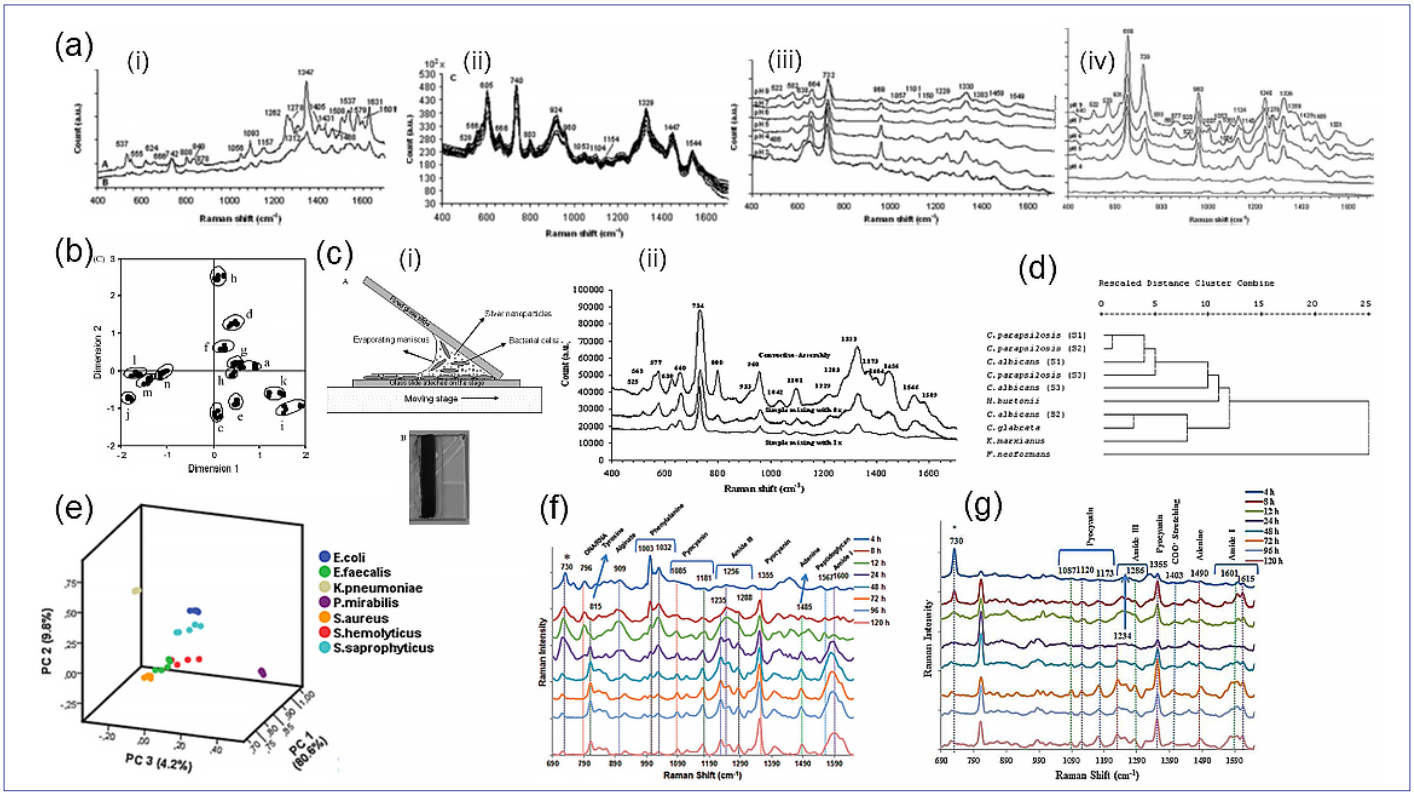

Figure 3. (a) SERS spectra of E. coli acquired with a laser at a wavelength of 514 nm (i), of 830 nm (ii), changes of spectral features and intensity of Raman scattering with pH change on E. coli (iii) and on B. megaterium (adapted from ref. 31). (b) Distribution of all bacterial SERS (binary and ternary mixtures) on the plot (adapted from ref. 32). (c) Convective assembly process of bacteria (i), Comparison of SERS spectrum of E. coli prepared with three methods (ii) (adapted from ref. 33). (d) Dendrogram constructed from the SERS data of ten yeast samples (adapted from ref. 34). (e) PCA plots of bacteria spectra at 1 h (adapted from ref. 36). (f) SERS spectra of biofilm formation of P. aeruginosa at different cultivation times between 4 and 120 h. (adapted from ref. 37). (g) SERS spectra of P. aeruginosa biofilm formation on 3D PMMA substrates at different cultivation times between 4 and 120 h. (adapted from ref. 38).

more changes in the spectral features of the Gram-positive bacteria, B. megaterium, with pH change. The increase in colloidal concentration in the mixture had a definite impact not only on the reproducibility but also on the spectral features of the spectra. Cam et al. showed multiplex identification of bacteria in bacterial mixtures with SERS.[32] The binary and ternary mixture of three different but related bacterial species Shigella sonnei, Proteus vulgaris, and Erwinia amylovara and three Escherichia coli strains (BFK13, BHK7, DH5 α) were used as model systems to test the feasibility of the approach. Acquired spectra from mixtures were analyzed using Euclidian distance charts and differentiation of each mixture were demonstrated. Kahraman et al. developed A sample preparation method based on convective assembly for "whole-microorganism" identification using SERS.[33] With this technique, a uniform sample can easily be prepared with silver nanoparticles. During the deposition process, bacteria and nanoparticles are assembled to form a unique well-ordered structure with great reproducibility. The SERS spectra acquired from the samples prepared with this technique have better quality and improved reproducibility for SERS spectra obtained from the same sample and limited variation due to the consistent sample preparation. E. coli, a Gram-negative bacillus, and Staphylococcus cohnii, a Gram-positive coccus, were studied as model bacteria. Sayin et al. characterized yeast species with SERS technique.[34] The sample for SERS analysis was prepared by mixing the yeast cells with a four times concentrated silver colloidal suspension. The scanning electron microscopy (SEM) images showed that the strength of the interaction between silver nanoparticles and the yeast cells depends on the biochemical structure of the cell wall. The SERS spectra were used to identify the biochemical structures on the yeast cell wall. It was found that the density of –SH and –NH_2 groups might be higher on certain yeast cell walls. Finally, the obtained SERS spectra from yeast was used for the classification of the yeast. In another study, Culha et al. identified yeast and bacteria in the presence of the other species.[35] Euclidian distance maps of the acquired spectra from single bacteria, single yeasts, and bacteria-yeast mixture showed clear differentiation. Avci et al. showed discrimination of urinary tract infection causative pathogens within 1 h of incubation using principal component analysis (PCA) of SERS spectra of seven different UTI causative bacterial species.[36] In addition, we showed differentiation of them at their different growth phases. We also analyzed origins of bacterial SERS spectra and demonstrated the highly dynamic structure of the bacteria cell wall during their growth.

Biofilm is a system composed of microorganisms and extracellular polymeric substances (EPS) including lipids, proteins, polysaccharides, humic substances, and genetic materials. Kelestemur et al. monitored the biofilm formation of clinically important microorganisms, Pseudomonas aeruginosa, Staphylococcus epidermidis, and Candida albicans with SERS.[37] The SERS spectra were collected by mapping a dried droplet area where a volume of colloidal silver nanoparticle (AgNP) suspension is placed on microorganism culture plate. The spectral changes on the SERS spectra with increasing incubation time of the model microorganisms from 4 to 120 h are monitored. The unique spectra originating from the biofilms of three pathogenic microorganisms and the spectral changes as a result of time-dependent concentration fluctuations of biomolecular species in their biofilms including carbohydrates, lipids, proteins, and genetic materials allow not only identification but also discrimination of biofilms using principal component analysis. In another study, we also investigated biofilm formation on 2-dimensional (2D) and 3-dimensional (3D) PMMA substrates to understand the influence of surface structures and also to demonstrate the discrimination of microorganisms according to their metabolic activities by utilizing SERS.[38] It was found that the fibrous 3D structure enhanced the assembly of microorganisms and enriched the biofilm structure while smooth polymeric surface decreased the biofilm formation rate and variety of biofilm content. Among the studied microorganisms, Pseudomonas aeruginosa and Candida albicans had a higher tendency to form biofilm on both 2D and 3D PMMA substrates. Although Staphlylococcus epidermidis showed slow adaption on PMMA surfaces, the 3D porous surfaces increased its biofilm formation rate significantly compared to 2D surface.

Eukaryotic Cells

SERS has started to gain attention in single-cell analysis due to its distinct advantages such as higher sensitivity and nondestructive nature by providing clearer potential answers to the challenging questions compared to the conventional techniques. Critical information can be extracted from the changes in conformation or abundancy of biomolecules during cellular dynamics and chemical milieu at stimulated or other various conditions such as cell division and apoptosis. These properties of label-free SERS make it different from many other conventional molecular biological detection tools because, unlike a Western-blot analysis, the expression level of a specific protein cannot be obtained from a label-free SERS spectrum. Thus, the technique provides an alternative approach to the biological information. Even though extracting organelle-specific information may not be possible with label-free SERS, the overall real-time cellular dynamics in a cell can be monitored, which is not possible to the same extent when only one type of conventional molecular biology assay is utilized at a time or when other single-cell analysis approaches are applied.

What label-free SERS can "see" in a cell is a combination of bonds present in biomacromolecules, which requires the pre-knowledge of the cellular localization and aggregation status as well as the chemical environment of the SERS substrate for the interpretation. At this point, the surface and microenvironment of SERS substrate require special attention. Therefore, the future research should focus on the AuNP surface characteristics, from the point the substrates are added into the culture medium to their localization within cells as well as the origins of the spectral bands to enhance the power of SERS in biological applications.

The biochemical processes taking place in endolysosomal vesicles cannot be considered independent of processes occurring in other locations of a cell. Because the SERS substrates are mostly found to reside in these vesicles, the acquired spectral information reflects the composition and cellular processes in there. Understanding the relationship between SERS spectra and biochemical processes in the endolysosomal vesicles is a clear research direction. Future studies should also focus on dynamics and content in endolysosomal vesicles by studying the processes through conventional techniques to relate the spectral patterns and changes to the molecular changes taking place in the vesicles. The information that will be obtained from such studies can then be correlated to results obtained in single cell SERS studies to provide further reliability on spectral interpretation.

Furthermore, to build up a healthy database of living single cell SERS studies, the reports should also include all the relevant information including the cellular localization of SERS substrates, the amount and type of spectral acquisitions from a cell, as well as the number of cells scanned in the reported studies.

Kuku et al. report a novel approach for nanotoxicity evaluation based on SERS.[39] Three model nanomaterials (ZnO nanoparticles, TiO_2 nanoparticles, and single-walled carbon nanotubes) were tested on two model cell lines (A549-human Caucasian lung carcinoma and HSF-human skin fibroblast) and the results were validated by WST-1 cytotoxicity assay and annexin

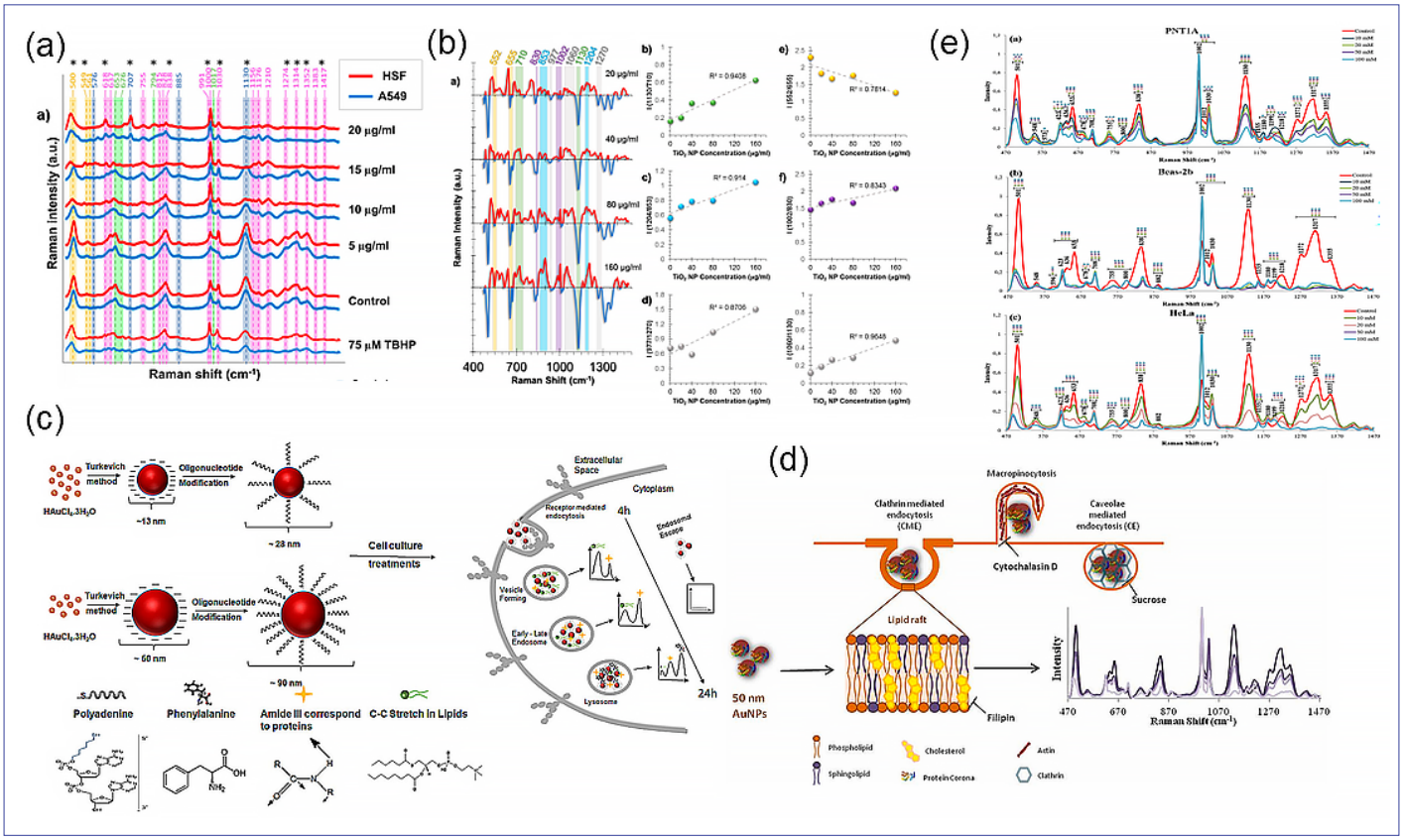

Figure 4. (a) SERS spectra of HSF (red) and A549 (blue) cells incubated with increasing concentrations of ZnO NPs were compared to nontreated control cells as well as 75 µM TBHP-treated positive control (adapted from ref. 39). (b) The spectra obtained from non-incubated control cells were subtracted from the TiO_2 NP-incubated cells and related peak analyses for different molecular changes between two groups (adapted from ref. 40). (c) Graphical abstract figure for the overview of the findings (adapted from ref. 41). (d) Graphical abstract figure for the overview of the findings (adapted from ref. 42). (e) Average SERS spectra of (a) PNT1A, (b) Beas-2b, and (c) HeLa cells treated with 10-, 20-, 50-, and 100-mM dG (adapted from ref. 43).

V-FITC/propidium iodide (PI) staining as apoptosis-necrosis assay. The localization of nanoparticles in the cells and the cellular conditions upon nanoparticle incubation were visualized by transmission electron microscopy (TEM) and enhanced dark-field (EDF) microscopy. SERS revealed a broader view on the consequences of cell–nanomaterial interactions compared to the conventional cytotoxicity assays where only one aspect of toxicity can be measured by one assay type. The results suggest that SERS can significantly contribute to the cytotoxicity evaluation bypassing nanomaterials or assay component-related complications with less effort. In another work, Kuku et al. investigated the origins of toxic response to TiO_2 nanoparticles of three different cell lines.[40] Vein (HUVEC), lung carcinoma (A549) and skin (L929) origin cell lines were tested for their toxic response upon exposure to 20, 40, 80 and 160 µg/mL anatase-TiO_2 nanoparticles for 24 h. It was demonstrated that the level of toxic response is both cell line and dose-dependent. L929 fibroblasts were the most resistant cell line to oxidative stress whereas in HUVEC and A549, cell lines collagen and lipid deformation were observed, respectively. Oztas et al. investigated endosomal biochemical dynamics based on size and surface chemistry-dependent uptake of gold nanoparticles (AuNPs) on single cells over time using SERS.[41] MDA-MB-231 breast cancer cells were exposed to 13 and 50 nm AuNPs and their polyadenine oligonucleotide-modified forms by controlling the order and combination of AuNPs. The average spectra obtained from 20 single cells were analyzed to study the nature of the biochemical species or processes taking place on the AuNP surfaces. The spectral changes, especially from proteins and lipids of endosomal vesicles, were observed depending on the size, surface chemistry, and combination as well as the duration of the AuNP treatment. The results demonstrate that SERS spectra are sensitive to trace biochemical changes not only the size, surface chemistry, and aggregation status of AuNPs but also the endosomal maturation steps over time, which can be simple and fast way for understanding the AuNP behavior in single cell and useful for the assisting and controlling of AuNP-based gene or drug delivery applications. Yılmaz et al. studied the pathway dependent endocytosis of gold nanoparticles using three different inhibitors for each endocytosis pathway (macropinocytosis was blocked by cytochalasin D (CytoD), clathrin mediated endocytosis (CME) by sucrose (Scr), and caveolae mediated endocytosis (CE) by filipin (Fil) of three model cell lines Beas-2b, A549 and PNT1A.[42] The results showed that cell type dependent AuNPs internalization affects not only the response of the cells to the inhibitors but also the obtained SERS spectra. SERS spectra of PNT1A cells treated with inhibitors was influenced most. The inhibition of each endocytosis pathway significantly affected the SERS spectral pattern and the spectral changes in different endocytosis pathways were clearly discriminated from each other. This means that SERS can significantly contribute to the investigation of different endosomal pathways from single living cells without any disruption of the cells or labeling. In another study, Yılmaz et al. investigated receptor-mediated endocytosis with SERS by inhibiting endocytosis with ATP depletion agents: sodium azide (NaN_3) and 2-deoxy-d-glucose (dG). Human lung bronchial epithelium (Beas-2b) cells, normal prostate

epithelium (PNT1A) cells, and cervical cancer epithelium (HeLa) cells were used as models.[43] First, the effect of NaN_3 and dG on the cells were examined through cytotoxicity, apoptosis–necrosis, ATP assay, and uptake inhibition analysis. An attempt to relate the spectral changes in the cellular spectra to the studied cellular events, receptor-mediated endocytosis inhibition, was made. It was found that the effect of two different ATP depletion agents can be discriminated by SERS, and hence receptor-mediated endocytosis can be tracked from single living cells with the technique without using a label and with limited sample preparation.

Conclusions

In this paper, after a brief historical introduction of Raman Scattering, we summarized our effort to utilize SERS for medical and biomedical applications with some examples. We believe that SERS has enormous potential not only to help to decipher the code of biosystems but also to speed up detection and identification processes with a detection sensitivity at the single-molecule level, fast analysis time, and low cost, and thus can be considered as a promising alternative technique to the current conventional techniques.

References

1. Strutt, J. XXXVI. On the light from the sky, its polarization and colour. *The London, Edinburgh, and Dublin Philosophical Magazine and Journal of Science* **1871**, *41* (273), 274-279.
2. Strutt, J. W. XV. On the light from the sky, its polarization and colour. *The London, Edinburgh, and Dublin Philosophical Magazine and Journal of Science* **1871**, *41* (271), 107-120.
3. Strutt, J. W. LVIII. On the scattering of light by small particles. *The London, Edinburgh, and Dublin Philosophical Magazine and Journal of Science* **1871**, *41* (275), 447-454.
4. Rayleigh, L. X. On the electromagnetic theory of light. *The London, Edinburgh, and Dublin Philosophical Magazine and Journal of Science* **1881**, *12* (73), 81-101.
5. Rayleigh, L. XXXIV. On the transmission of light through an atmosphere containing small particles in suspension, and on the origin of the blue of the sky. *The London, Edinburgh, and Dublin Philosophical Magazine and Journal of Science* **1899**, *47* (287), 375-384.
6. Raman, C. V. On the molecular scattering of light in water and the colour of the sea. *Proc. R. Soc. Lond. A* **1922**, *101* (708), 64-80.
7. Compton, A. H. A quantum theory of the scattering of X-rays by light elements. *Physical review* **1923**, *21* (5), 483.
8. Raman, C. V.; Krishnan, K. S. A new type of secondary radiation. *Nature* **1928**, *121* (3048), 501.
9. Tuschel D. Raman thermometry. *Spectroscopy Online* 2016.
10. Ritchie, R. H. Plasma losses by fast electrons in thin films. *Physical Review* **1957**, *106* (5), 874.
11. Barnes, W. L.; Dereux, A.; Ebbesen, T. W. Surface plasmon subwavelength optics. *Nature* **2003**, *424* (6950), 824.
12. Maier, S. A.; Atwater, H. A. Plasmonics: Localization and guiding of electromagnetic energy in metal/dielectric structures. *Journal of applied physics* **2005**, *98* (1), 10.
13. Kelly, K. L.; Coronado, E.; Zhao, L. L.; Schatz, G. C. The optical properties of metal nanoparticles: the influence of size, shape, and dielectric environment. *J. Phys. Chem. B,* **2003**, 107 (3), 668-677.
14. Sosa, I. O.; Noguez, C.; Barrera, R. G. Optical properties of metal nanoparticles with arbitrary shapes. *The Journal of Physical Chemistry B* **2003**, *107* (26), 6269-6275.
15. Stiles, P. L.; Dieringer, J. A.; Shah, N. C.; Van Duyne, R. P. Surface-enhanced Raman spectroscopy. *Annu. Rev. Anal. Chem.* **2008**, *1*, 601-626.
16. Fleischmann, M.; Hendra, P. J.; McQuillan, A. J. Raman spectra of pyridine adsorbed at a silver electrode. *Chemical Physics Letters* **1974**, *26* (2), 163-166.
17. Jeanmaire, D. L.; Van Duyne, R. P. Surface Raman spectroelectrochemistry: Part I. Heterocyclic, aromatic, and aliphatic amines adsorbed on the anodized silver electrode. *Journal of electroanalytical chemistry and interfacial electrochemistry* **1977**, *84* (1), 1-20.
18. Albrecht, M. G.; Creighton, J. A. Anomalously intense Raman spectra of pyridine at a silver electrode. *Journal of the american chemical society* **1977**, *99* (15), 5215-5217.
19. Van Duyne, R. Raman applications of Raman spectroscopy in electrochemistry. *Le Journal de Physique Colloques* **1977**, *38* (C5), C5-239-C235-252.
20. Kleinman, S. L.; Frontiera, R. R.; Henry, A.-I.; Dieringer, J. A.; Van Duyne, R. P. Creating, characterizing, and controlling chemistry with SERS hot spots. *Physical Chemistry Chemical Physics* **2013**, *15* (1), 21-36.
21. Fang, Y.; Seong, N.-H.; Dlott, D. D. Measurement of the distribution of site enhancements in surface-enhanced Raman scattering. *Science* **2008**, *321* (5887), 388-392.
22. Stranahan, S. M.; Willets, K. A. Super-resolution optical imaging of single-molecule SERS hot spots. *Nano letters* **2010**, *10* (9), 3777-3784.
23. Ross, M. B.; Ashley, M. J.; Schmucker, A. L.; Singamaneni, S.; Naik, R. R.; Schatz, G. C.; Mirkin, C. A. Structure–function relationships for surface-enhanced Raman spectroscopy-active plasmonic paper. *The Journal of Physical Chemistry C* **2016**, *120* (37), 20789-20797.
24. Culha M. Surface-enhanced Raman scattering: an emerging label-free detection and identification technique for proteins. *Applied Spectroscopy* **2013**, 67, 355-364.
25. Kitahama, Y.; Ozaki, Y. Surface-enhanced resonance Raman scattering of hemoproteins and those in complicated biological systems. *Analyst* **2016**, 141, 5020-5036.
26. Das, G.; Gentile, F.; Coluccio, M; Perri, A; Nicastri, A; Mecarini, F; Cojoc, G; Candeloro, P; Liberale, C; De Angelis, F. Principal component analysis based methodology to distinguish protein SERS spectra. *J Mol Struct* **2011**, 993, 500-505.
27. Avci, E.; Culha, M. Influence of protein size on surface-enhanced Raman scattering (SERS) spectra in binary protein mixtures. *Applied Spectroscopy* **2014**, *68* (8), 890-899.
28. Kahraman, M.; Sur, I.; Çulha, M. Label-free detection of proteins from self-assembled protein-silver nanoparticle structures using surface-enhanced Raman scattering. *Analytical chemistry* **2010**, *82* (18), 7596-7602.
29. Keskin, S.; Kahraman, M.; Çulha, M. Differential separation of protein mixtures using convective assembly and label-free detection with surface enhanced Raman scattering. *Chemical Communications* **2011**, *47* (12), 3424-3426.
30. Keskin, S.; Çulha, M. Label-free detection of proteins from dried-suspended droplets using surface enhanced Raman scattering. *Analyst* **2012**, *137* (11), 2651-2657.
31. Kahraman, M.; Yazici, M. M.; Şahin, F.; Bayrak, Ö. F.; Çulha, M. Reproducible surface-enhanced Raman scattering spectra of bacteria on aggregated silver nanoparticles. *Applied spectroscopy* **2007**, *61* (5), 479-485.
32. Cam, D.; Keseroglu, K.; Kahraman, M.; Sahin, F.; Culha, M. Multiplex identification of bacteria in bacterial mixtures with surface-enhanced Raman scattering. *Journal of Raman Spectroscopy: An International Journal for Original Work in all Aspects of Raman Spectroscopy, Including Higher Order Processes, and also Brillouin and Rayleigh Scattering* **2010**, *41* (5), 484-489.
33. Kahraman, M.; Yazıcı, M. M.; Şahin, F.; Çulha, M. Convective assembly of bacteria for surface-enhanced Raman scattering. *Langmuir* **2008**, *24* (3), 894-901.
34. Characterization of yeast species using surface-enhanced Raman scattering. *Applied spectroscopy* **2009**, *63* (11), 1276-1282.
35. Culha, M.; Kahraman, M.; Çam, D.; Sayın, I.; Keseroğlu, K. Rapid identification of bacteria and yeast using surface-enhanced Raman scattering. *Surface and Interface Analysis* **2010**, *42* (6-7), 462-465.
36. Avci, E.; Kaya, N. S.; Ucankus, G.; Culha, M. Discrimination of urinary tract infection pathogens by means of their growth profiles using surface enhanced Raman scattering. *Analytical and bioanalytical chemistry* **2015**, *407*, 8233-8241.
37. Keleştemur, S.; Çulha, M. Understanding and discrimination of biofilms of clinically relevant microorganisms using surface-enhanced Raman scattering. *Applied Spectroscopy* **2017**, *71* (6), 1180-1188.
38. Keleştemur, S.; Çobandede, Z.; Çulha, M. Biofilm formation of clinically important microorganisms on 2D and 3D poly (methyl methacrylate) substrates: A surface-enhanced Raman scattering study. *Colloids and Surfaces B: Biointerfaces* **2020**, *188*, 110765.
39. Kuku, G.; Saricam, M.; Akhatova, F.; Danilushkina, A.; Fakhrullin, R.; Culha, M. Surface-enhanced Raman scattering to evaluate nanomaterial cytotoxicity on living cells. *Analytical chemistry* **2016**, *88* (19), 9813-9820.
40. Kuku, G.; Culha, M. Investigating the origins of toxic response in TiO2 nanoparticle-treated cells. *Nanomaterials* **2017**, *7* (4), 83.
41. Öztaş, D. Y.; Altunbek, M.; Uzunoglu, D.; Yılmaz, H. I.; Çetin, D.; Suludere, Z.; Çulha, M. Tracing size and surface chemistry-dependent endosomal uptake of gold nanoparticles using surface-enhanced Raman scattering. *Langmuir* **2019**, *35* (11), 4020-4028.
42. Yılmaz, D.; Culha, M. Investigation of the pathway dependent endocytosis of gold nanoparticles by surface-enhanced Raman scattering. *Talanta* **2021**, *225*, 122071.
43. Yılmaz, D.; Culha, M. Discrimination of receptor-mediated endocytosis by surface-enhanced raman scattering. *Langmuir* **2022**, *38* (20), 6281-6294.